

Spectral characterization and performance of SPT-SLIM on-chip filterbank spectrometers

C. S. Benson[‡], K. Fichman^{*†}, M. Adamic[§], A. J. Anderson^{¶†||}, P. Barry[‡], B. A. Benson^{¶†||}, E. Brooks^{||}, J. E. Carlstrom^{†***††||}, T. Cecil^{††}, C. L. Chang^{†††||}, K. R. Dibert^{||}, M. Dobbs[§], K. S. Karkare^{‡‡}, G. K. Keating^x, A. M. Lapuente^{‡‡}, M. Lisovenko^{††}, D. P. Marrone^{xi}, J. Montgomery[§], T. Natoli[†], Z. Pan^{†††*}, A. Rahlin^{||†}, G. Robson[‡], M. Rouble[§], G. Smecher^{xiii§}, V. Yefremenko^{††}, M. R. Young^{¶†}, C. Yu^{†††||}, J. A. Zebrowski^{†||¶}, C. Zhang^{xiii}, *Department of Physics, University of Chicago, 5640 South Ellis Avenue, Chicago, IL, 60637, USA [†]Kavli Institute for Cosmological Physics, University of Chicago, 5640 South Ellis Avenue, Chicago, IL, 60637, USA [‡]School of Physics and Astronomy, Cardiff University, Cardiff CF24 3YB, United Kingdom [§]Department of Physics and Trottier Space Institute, McGill University, 3600 Rue University, Montreal, Quebec H3A 2T8, Canada [¶]Fermi National Accelerator Laboratory, MS209, P.O. Box 500, Batavia, IL, 60510, USA ^{||}Department of Astronomy and Astrophysics, University of Chicago, 5640 South Ellis Avenue, Chicago, IL, 60637, USA ^{**}Enrico Fermi Institute, University of Chicago, 5640 South Ellis Avenue, Chicago, IL, 60637, USA ^{††}High-Energy Physics Division, Argonne National Laboratory, 9700 South Cass Avenue., Lemont, IL, 60439, USA ^{‡‡}Department of Physics, Boston University, 590 Commonwealth Avenue, Boston, MA, 02215, USA ^xHarvard-Smithsonian Center for Astrophysics, 60 Garden Street, Cambridge, MA, 02138, USA ^{xi}Steward Observatory and Department of Astronomy, University of Arizona, 933 N. Cherry Ave., Tucson, AZ 85721, USA ^{xii}Three-Speed Logic, Inc., Victoria, B.C., V8S 3Z5, Canada ^{xiii}SLAC National Accelerator Laboratory, 2575 Sand Hill Road, Menlo Park, CA, 94025, USA

Abstract—The South Pole Telescope Shirokoff Line Intensity Mapper (SPT-SLIM) experiment is a pathfinder for demonstrating the use of on-chip spectrometers for millimeter (mm) Line Intensity Mapping (LIM). We present spectral bandpass measurements of the SLIM spectrometer channels made on site using a Fourier Transform Spectrometer during SPT-SLIMs first deployment the 2024-2025 austral summer observing season. Through this we demonstrate a technique for measuring the narrow band passes of the SPT-SLIM filterbanks that improves beyond the intrinsic resolution of a Fourier Transform Spectrometer.

I. INTRODUCTION

Line Intensity Mapping (LIM) uses imaging spectroscopy to trace emission lines as a function of redshift, producing three-dimensional spatial/spectral maps of the large scale structure (LSS) in the Universe without needing to spatially resolve individual sources. In comparison to galaxy surveys, LIM can access larger volumes of space and higher redshifts. LIM in the sub-millimeter/millimeter-wavelength band can provide constraints on cosmology, including expansion history [1] and the neutrino properties, effective number of neutrino species and the sum of the neutrino masses [2]. While it has significant potential, sub-millimeter/millimeter (sub-mm/mm) LIM is still maturing. Significant advancements in the sensitivity and scalability of large field-of-view mapping spectrometers are needed for sub-mm/mm LIM experiments to be competitive with and complementary to modern galaxy surveys.

SPT-SLIM is a pathfinder LIM experiment leveraging integrated on-chip filterbank spectrometers to place constraints on the CO power spectrum in the 120-180 GHz range from the SPT. SPT-SLIM targets CO(2-1) between $0.3 < z < 0.9$,

CO(3-2) between $0.8 < z < 1.8$, and CO(4-3) between $1.6 < z < 2.8$ [3]. SPT-SLIM deployed in the austral summer of 2024-2025 on the SPT in the camera position occupied by the Event Horizon Telescope (EHT) very-long-baseline interferometry (VLBI) receiver [4]. SPT is an ideal telescope for mm-wave LIM, as the high-altitude, low humidity, and stable weather at its location limit atmospheric noise [5]. The first deployment of SPT-SLIM has primarily focused on instrumentation and technology demonstration. Bright calibration sources, such as RCW-38 and the Moon, were prioritized to characterize the instrument. Future deployments will have updated detectors and will target a measurement of CO emission lines for LIM science.

To reconstruct the redshift dimension of the LIM signal, constrain atmospheric contamination, and disentangle interloper spectral features, reliable spectral response measurements of SPT-SLIM's spectral channels are crucial. This work gives an overview of the SPT-SLIM detector design and details the spectral characterization of the SPT-SLIM spectrometers during the first SPT-SLIM deployment. We demonstrate measurements of the central frequencies and spectral bandpasses with suitable accuracy beyond the intrinsic resolution of the on-site Fourier Transform Spectrometer (FTS) via spatial-domain fitting of the FTS measurements [6], [7].

As a companion to this work, details on the SPT-SLIM Adiabatic Demagnetization Refrigerator (ADR) used in the deployment are given in Young et al. (2025) [8]. Additionally, details on the RF-ICE detector readout system can be found in Rouble et al. (2022) [9].

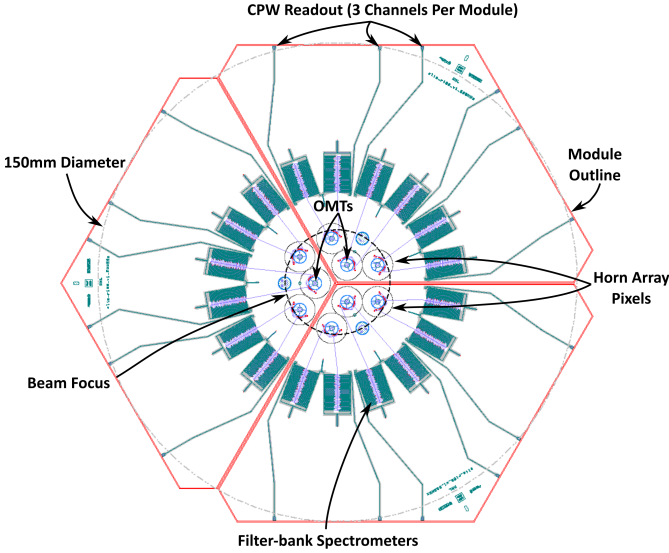


Fig. 1: A schematic diagram of the full SPT-SLIM focal plane [13].

II. SPT-SLIM: A FILTERBANK SPECTROMETER

In the SPT-SLIM design, light is coupled onto polarization sensitive orthomode transducers (OMTs) via gold-plated conical feedhorns [10], [11]. The OMTs are patterned on a thin film and mounted on an aluminum base with $\lambda/4$ backshort features. Each polarization mode of the OMT is coupled via a niobium microstrip transmission line to its own filterbank [12]. Each of the two filterbanks per antenna consist of 65 half-wave resonator filters capacitively coupled to the transmission line. Each filter provides a narrow spectral bandpass at a set frequency of light, with spectral resolution $R = \nu/\Delta\nu$, that then terminates on a Kinetic Inductance Detector (KID). SPT-SLIM uses a Lumped Element KID (LEKID) design with aluminum inductors and niobium interdigitated capacitors. All LEKIDs within a filterbank are coupled to a single microstrip readout line [13]. In addition to the narrow-band detectors that build up the spectrometer, each filterbank has three broadband detectors, and two dark detectors to assist in performance characterization. The dark detectors have no optical coupling to the filterbank transmission line. The SPT-SLIM focal plane consists of three wafers, called “submodules”, each with three readout lines, six filterbanks (one per polarization), and three antennae (see Fig. 1). Due to a combination of damage to the thin film OMTs and non-operational readout lines, five of the nine lines were operational for this first deployment. For additional details on the simulation, design, and fabrication of SPT-SLIM, see Barry et al. (2022) [12], Robson (2024) [13], Robson et al. (2022) [14], and Cecil et al (2023) [15].

SPT-SLIM adds to the burgeoning landscape of on-chip filterbank spectrometers. SPT-SLIM builds on the design and laboratory testing of SuperSpec [16] which has been successfully demonstrated through lab measurements [17] providing a multi-pixel on-sky demonstration of the technique in the 255–278 GHz range. SPT-SLIM also complements the single-pixel DEep Spectroscopic High-redshift MApper (DESHIMA) experiment, operating on-sky in the 220–440 GHz range [18].

III. MEASUREMENT

Characterization of the bandpasses of the SPT-SLIM experiment requires both accurate determination of band centers and bandpass shape. An FTS is an interferometer capable of measuring the spectral response of the filterbank spectrometers with an excellent absolute frequency calibration, but with frequency resolution limited by the size of the FTS. A measurement is performed by moving a mirror on a motorized platform at a constant speed, varying the differential path length and introducing a phase difference between a stationary arm and the moving arm of the interferometer. The resulting interference signal (i.e., interferogram) measured by the detectors is the Fourier transform of the detector spectra. Here we note that spectroscopic wavenumbers $\sigma = \frac{1}{\lambda} = \frac{\nu}{c}$, where c is the speed of light and ν is spectral frequency in units of inverse time, provides a natural frequency unit for FTS measurements. The focal plane was measured with the on-site FTS at the South Pole having a minimum resolution element of $d\nu \sim 6$ GHz, corresponding to $R = 25$ at 150 GHz, limited by optical systematics [19]. Additionally, we note that the minimum resolvable spectral resolution element, $\Delta\nu$, is constant across the spectral band.

The SPT-SLIM spectrometers have a design resolution of $R \sim 100$, significantly greater than that of the FTS at the South Pole. As a result, the spectrometer channel bandpasses are unresolved and broadened by the instrumental line shape of the low resolution FTS. Measuring the bandpasses from the spectrum retrieved by the FTS would provide a biased measurement of the filterbank R (see Fig. 2). We demonstrate that an accurate measurement of an under-resolved filter bandpass can be obtained by relying on the assumed spectral profile of the filters. A least-squares fit of the simulated detector signal measured in the spatial displacement domain of the FTS is used to extract the filter resolution and central frequency. For this, we have used the functional form of a Fourier-transformed Lorentzian (the corresponding profile of a half-wave filter),

$$I(z) = e^{-\sigma_0 \pi z / R} \cos(2\pi \sigma_0 z), \quad (1)$$

where σ_0 is the central spectral frequency of the band-pass in wavenumbers and z is optical path difference.

Fig. 3 demonstrates this technique for an SPT-SLIM filter channel measured by the low-resolution FTS at the South Pole. The top panel shows that the interference signal is well fit to within the approximate uncertainty of the technique (see Fig. 4) in the spatial domain. In the Fourier domain, the spectral profile measured directly with the FTS is smeared out by the ~ 6 GHz-wide line shape of the FTS while the Fourier transform of the functional form fitted in the spatial domain recovers a narrower, unbiased spectral profile (Fig 3, bottom panel).

To determine the accuracy of this technique, the fit was performed on simulated FTS data that incorporates a detector noise model. Model FTS measurements were generated with a variety of noise levels and while truncating the simulated interferogram to different FTS resolutions (note that the resolution of an FTS is determined by the maximum optical path difference measured) [20]. The extracted parameters from the

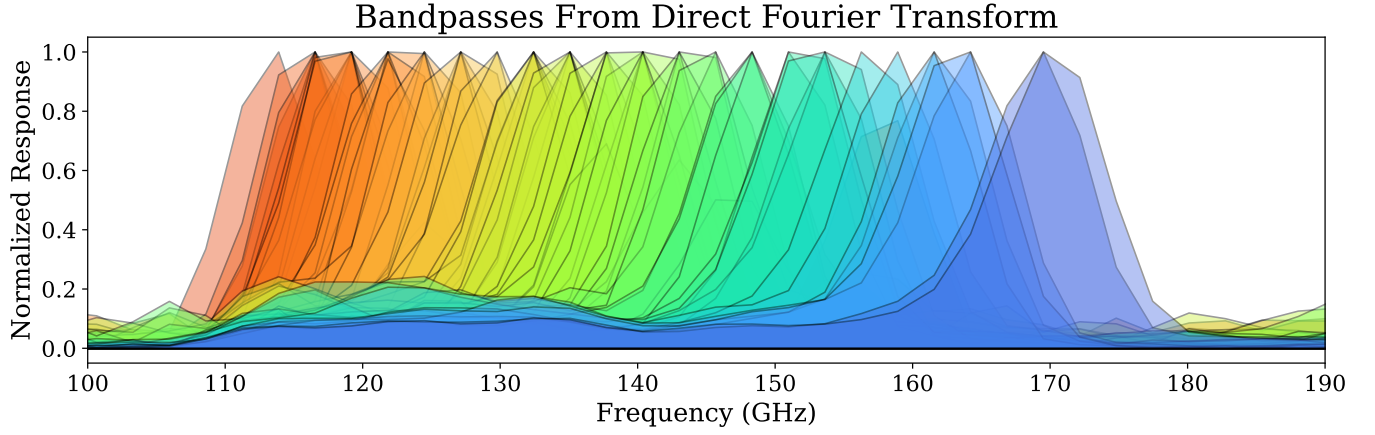


Fig. 2: The spectral channels of a polarisation-pair of deployment SPT-SLIM filterbanks measured with the FTS. Note that the width of each filter profile has been broadened by the instrumental line shape of the lower-resolution $\Delta\nu \sim 6$ GHz FTS.

fitting are compared against their simulated values in Fig. 4. For measurements with any reasonable signal-to-noise ratio (SNR), an FTS with an instrumental resolution that is greater than 20% of the filter resolution is all that is needed to accurately extract the central frequency of the band to within less than 0.2%. Similarly, for SNRs greater than 8, an FTS with 1/4 the resolution of an $R = 100$ filter is sufficient to measure the resolution of the filter to within $\sim \pm 10$. We also note that for any reasonable range of spatial sampling rates for the FTS used at the South Pole, providing more than $100\times$ Nyquist sampling over the range of interference signals in the spectral range of the SLIM band, the accuracy of the fit is unaffected.

Due to the interaction with other filters in the spectrometer, we expect the Lorentzian band-pass of a single filter to experience some asymmetry [13]. Despite the broadening from the FTS line profile, this can be seen in the measured spectral profile shown in Fig. 3 (lower panel). To account for this, we introduced a skew to the simulated data of the form

$$S(\sigma) = \frac{2\tau}{1 + 2\pi i\tau(\sigma - \sigma_0)} \left(1 + \frac{\alpha}{\tau}(\sigma - \sigma_0)\right), \quad (2)$$

where $\tau = R/(\pi\sigma_0)$ and α is the introduced skew parameter (see Fig. 5). For values ranging $|\alpha| = 0-10\tau$ with a SNR of 10, we have found that the asymmetry does not significantly affect the bias in values of σ_0 and R extracted from spatial-domain fits.

IV. FREQUENCY SCHEDULING AND RESOLUTION

Spatial-domain fitting was applied to the FTS measurements of both SPT-SLIM submodules that were operational for its first deployment at the SPT. All three lines on either submodule were measured, although one was not operational for on-sky measurements. These results are shown in Fig. 6. These measurements show a median spectral resolution of 33 ± 9 for both deployment submodules, below the design target of $R \approx 100$. We have taken a conservative uncertainty estimate of ± 9 in R , corresponding to the bias from the simulated results in Fig. 4 for the mean SNR of the filters in

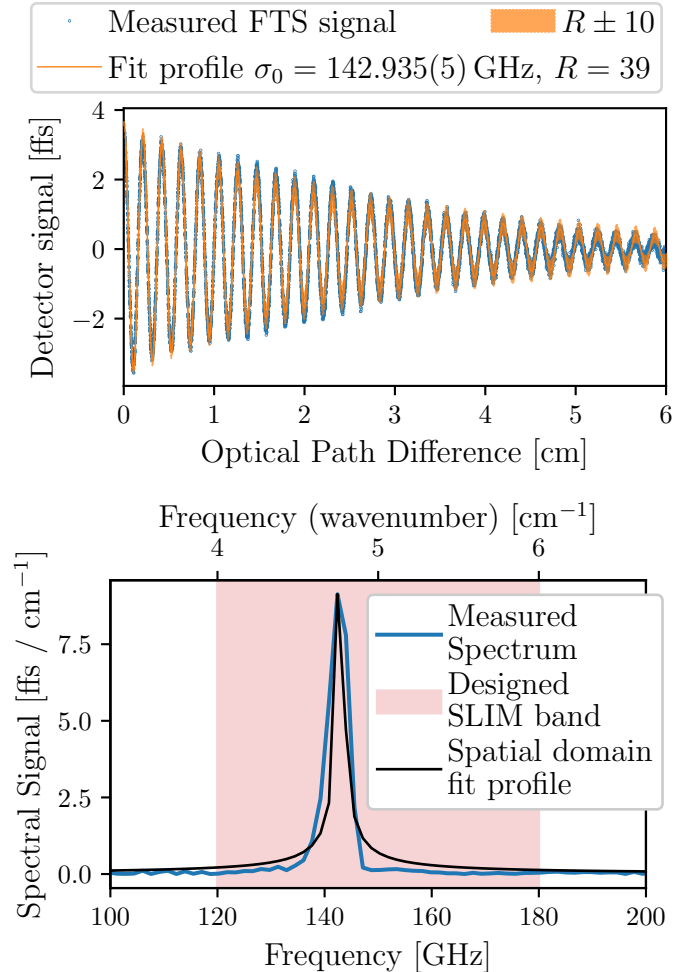


Fig. 3: A spatial-domain fit of the interference signal from one of the SLIM detectors (top). The spectrum of the corresponding spectrometer channel measured by the FTS and the spectral profile obtained from the spatial-domain fit are shown in the spectral (Fourier) domain (bottom). Note that the measured profile is smeared to a wider spectral bandpass due to the instrumental line shape of the low-resolution FTS.

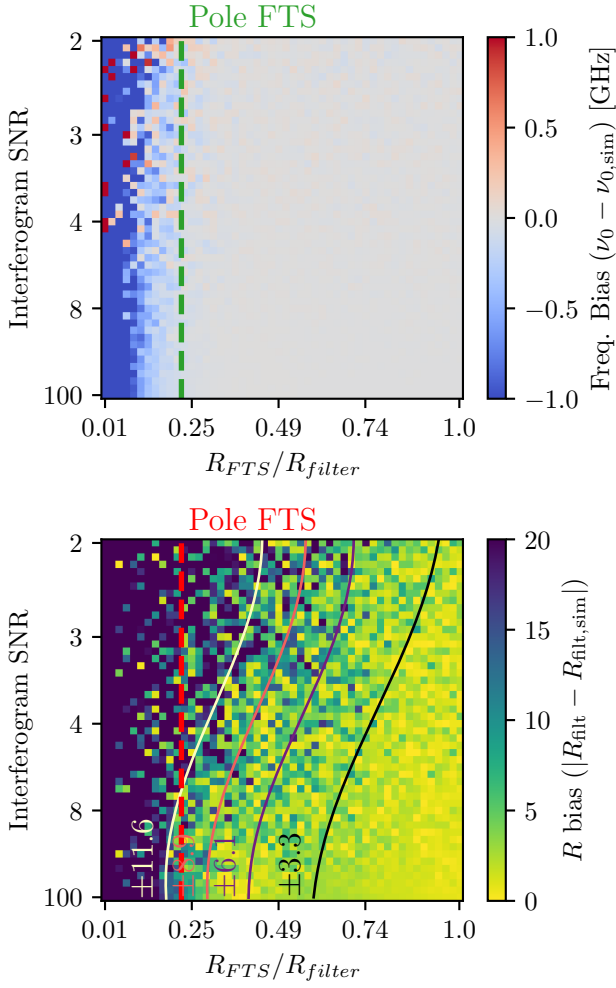


Fig. 4: The uncertainty in measurements of the central frequency (top) and spectral resolution/bandpass (bottom) of a filter extracted from spatial-domain fitting using simulated FTS measurements (see Eqs. 1–3). Simulated measurements were generated with a detector noise model at different signal-to-noise ratios (SNRs) and at different FTS resolving powers. In each case, the ratio of the resolving power of the South Pole FTS at 150 GHz to the $R = 100$ simulated filter resolution is marked by a vertical dashed line.

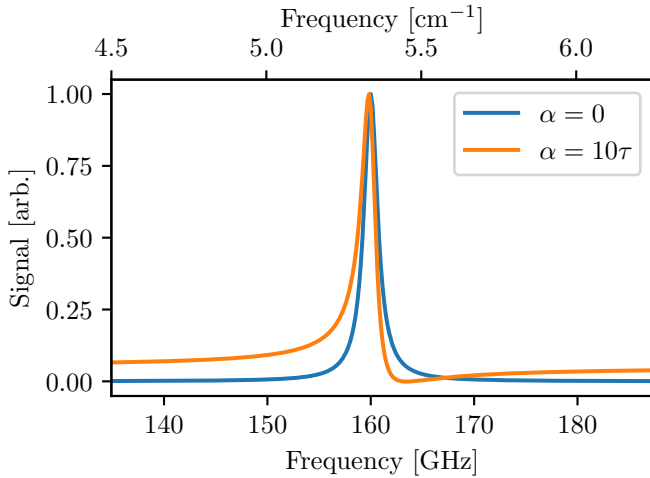


Fig. 5: The simulated spectral band pass of a filter with and without a modeled asymmetry (see Eq. 2).

each submodule. Additionally, the centers of the bandpasses are shifted downward from the target SLIM band by ~ 10 GHz.

Each spectral filter consists of a half-wave resonator connected to the transmission line and a detector via coupling capacitors which set the central frequency of the filter's transmission (see Fig. 7). This was tuned primarily by the physical dimensions of the filter and coupling capacitors and informed by simulations employing projected fabrication errors and an anticipated dielectric loss tangent for SiN [14]. The shift to lower frequency in the SPT-SLIM bands suggests a systematic deviation from our simulated results that is under study for the next generation of SPT-SLIM spectrometers.

The resolution of a filter is governed by the joined quality factors of the filter's coupling to the feedline Q_{feed} , the detector coupling, Q_{det} , and losses in the resonator Q_{loss} ,

$$\frac{1}{R} = \frac{1}{Q_{\text{filt}}} = \frac{1}{Q_{\text{feed}}} + \frac{1}{Q_{\text{det}}} + \frac{1}{Q_{\text{loss}}}. \quad (3)$$

In SPT-SLIM, Q_{feed} and Q_{det} are largely controlled by the dimensions of the capacitors that couple the half-wave resonator to the feedline and to the detector, respectively. We expect Q_{loss} to be dominated by the dielectric loss tangent ($\tan \delta$) of the SiN employed in the microstrip architecture.

The coupling quality factors of SPT-SLIM were designed to provide an $R = 100$ spectrometer with $\tan \delta = 1 \times 10^{-3}$. For these coupling quality factors, the resolution measurements in Fig. 6 would suggest a $\tan \delta \sim 2 \times 10^{-2}$. This greatly exceeds what has been measured in characterization experiments of Argonne SiN and optical measurements of test structures on deployment SLIM submodule wafers [13], [21]. As such, the low resolution of the deployment SPT-SLIM submodules is likely a consequence of both poor dielectric performance and capacitor fabrication.

The dielectric loss tangent of the SPT-SLIM structures compromises its performance in nearly every aspect, reducing optical efficiency, resolution, and increasing optical loading from the atmospheric emission lines that bookend the SLIM band.

V. CONCLUSION

In the 2024-2025 austral summer, SPT-SLIM deployed on the SPT in the camera position occupied by the EHT VLBI receiver. This deployment included 5 operational dual-polarization filterbank spectrometers. These spectrometers were characterized on site with a low-resolution FTS. We demonstrate a technique by which the spectral bandpass/resolution of the filters can be measured with an FTS having less than a quarter the resolution of the designed filter bandwidth. With this, the SPT-SLIM filterbanks deployed were measured to have an average spectral resolution $R = 34$, lower than the target resolution of $R = 100$. This is likely caused by differences between the simulated and fabricated dielectrics, in which lossy dielectric lowers the resolution from design. These measured bandpasses are applied to observations of the atmosphere and moon in Dibert et al. [22].

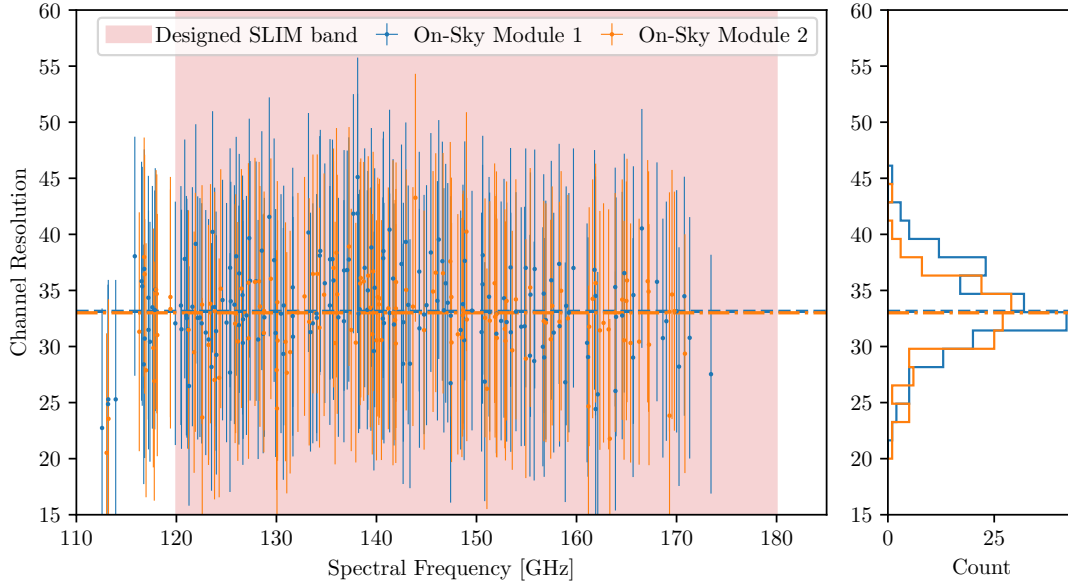


Fig. 6: The fitted resolution, R , of the on-sky submodules extracted from measurements with the South Pole FTS (see Eq. 3). Error bars represent the biases determined from the simulated data shown in Fig. 4 at the corresponding SNR of the interferogram measured with the FTS.

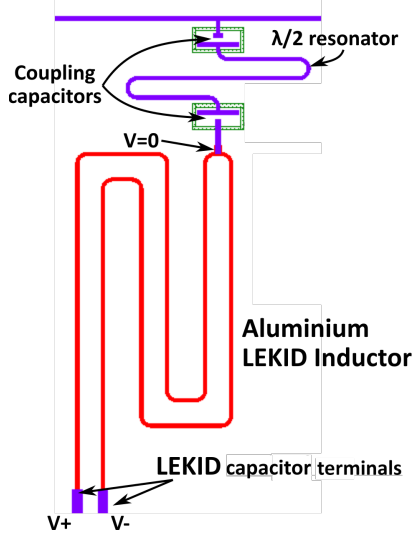


Fig. 7: A diagram of a single SPT-SLIM channel. Each filter (i.e., half-wave resonator) is capacitively coupled to the transmission line from the OMT and terminates in a capacitive coupled LEKID. Adapted from Robson (2024) [13].

VI. ACKNOWLEDGMENTS

This work was supported by funding from the National Science Foundation, Fermilab National Laboratory under the Department of Energy, and the United Kingdom Research and Innovation.

REFERENCES

- [1] K. S. Karkare and S. Bird, “Constraining the expansion history and early dark energy with line intensity mapping,” *Physical Review D*, vol. 98, p. 043529, Aug. 2018.
- [2] A. Moradinezhad Dizgah, G. K. Keating, K. S. Karkare, A. Crites, and S. R. Choudhury, “Neutrino Properties with Ground-based Millimeter-wavelength Line Intensity Mapping,” *The Astrophysical Journal*, vol. 926, p. 137, Feb. 2022.
- [3] K. S. Karkare, A. J. Anderson, P. S. Barry, B. A. Benson, J. E. Carlstrom, T. Cecil, C. L. Chang, M. A. Dobbs, M. Hollister, G. K. Keating, D. P. Marrone, J. McMahon, J. Montgomery, Z. Pan, G. Robson, M. Rouble, E. Shirokoff, and G. Smecher, “SPT-SLIM: A Line Intensity Mapping Pathfinder for the South Pole Telescope,” *Journal of Low Temperature Physics*, vol. 209, pp. 758–765, Dec. 2022.
- [4] J. Kim, D. P. Marrone, C. Beaudoin, J. E. Carlstrom, S. S. Doeleman, T. W. Folkers, D. Forbes, C. H. Greer, E. F. Lauria, K. D. Massingill, E. Mayer, C. H. Nguyen, G. Reiland, J. SooHoo, A. A. Stark, L. Vertatschitsch, J. Weintraub, and A. Young, “A VLBI receiving system for the South Pole Telescope,” in *Millimeter, Submillimeter, and Far-Infrared Detectors and Instrumentation for Astronomy IX* (J. Zmuidzinas and J.-R. Gao, eds.), vol. 10708 of *Society of Photo-Optical Instrumentation Engineers (SPIE) Conference Series*, p. 107082S, July 2018.
- [5] J. E. Carlstrom, P. A. R. Ade, K. A. Aird, B. A. Benson, L. E. Bleem, S. Busetti, C. L. Chang, E. Chauvin, H. M. Cho, T. M. Crawford, A. T. Crites, M. A. Dobbs, N. W. Halverson, S. Heimsath, W. L. Holzapfel, J. D. Hrubes, M. Joy, R. Keisler, T. M. Lanting, A. T. Lee, E. M. Leitch, J. Leong, W. Lu, M. Lueker, D. Luong-Van, J. J. McMahon, J. Mehl, S. S. Meyer, J. J. Mohr, T. E. Montroy, S. Padin, T. Plagge, C. Pryke, J. E. Ruhl, K. K. Schaffer, D. Schwan, E. Shirokoff, H. G. Spieler, Z. Staniszewski, A. A. Stark, C. Tucker, K. Vanderlinde, J. D. Vieira, and R. Williamson, “The 10 Meter South Pole Telescope,” *Publications of the Astronomical Society of the Pacific*, vol. 123, p. 568, May 2011.
- [6] P. S. Barry, *On the development of SuperSpec: a fully integrated on-chip spectrometer for far-infrared astronomy*. PhD thesis, Cardiff University, UK, Jan. 2014.
- [7] S. Hailey-Dunsheath, P. S. Barry, C. M. Bradford, G. Chattopadhyay, P. Day, S. Doyle, M. Hollister, A. Kovacs, H. G. LeDuc, N. Lombart, P. Mauskopf, C. McKenney, R. Monroe, H. T. Nguyen, R. O’Brien, S. Padin, T. Reck, E. Shirokoff, L. Swenson, C. E. Tucker, and J. Zmuidzinas, “Optical Measurements of SuperSpec: A Millimeter-Wave On-Chip Spectrometer,” *Journal of Low Temperature Physics*, vol. 176, pp. 841–847, Sept. 2014.
- [8] M. Young and the SPT-SLIM Collaboration, “Cryogenic Performance of the SPT-SLIM Receiver,” *IEEE Transactions on Applied Superconductivity*, 2025. Submitted August 2025.
- [9] M. Rouble, G. Smecher, A. Anderson, P. S. Barry, K. Dibert, M. Dobbs, K. S. Karkare, and J. Montgomery, “RF-ICE: large-scale gigahertz readout of frequency-multiplexed microwave kinetic inductance detectors,” in *Millimeter, Submillimeter, and Far-Infrared Detectors and*

- Instrumentation for Astronomy XI* (J. Zmuidzinas and J.-R. Gao, eds.), vol. 12190 of *Society of Photo-Optical Instrumentation Engineers (SPIE) Conference Series*, p. 1219024, Aug. 2022.
- [10] K. W. Yoon, J. W. Appel, J. E. Austermann, J. A. Beall, D. Becker, B. A. Benson, L. E. Bleem, J. Britton, C. L. Chang, J. E. Carlstrom, H. Cho, A. T. Crites, T. Essinger-Hileman, W. Everett, N. W. Halverson, J. W. Henning, G. C. Hilton, K. D. Irwin, J. McMahon, J. Mehl, S. S. Meyer, S. Moseley, M. D. Niemack, L. P. Parker, S. M. Simon, S. T. Staggs, K. U-yen, C. Visnjic, E. Wollack, and Y. Zhao, "Feedhorn-coupled tes polarimeters for next-generation cmb instruments," *AIP Conference Proceedings*, vol. 1185, pp. 515–518, 12 2009.
 - [11] J. McMahon, J. W. Appel, J. E. Austermann, J. A. Beall, D. Becker, B. A. Benson, L. E. Bleem, J. Britton, C. L. Chang, J. E. Carlstrom, H. M. Cho, A. T. Crites, T. Essinger-Hileman, W. Everett, N. W. Halverson, J. W. Henning, G. C. Hilton, K. D. Irwin, J. Mehl, S. S. Meyer, S. Mossley, M. D. Niemack, L. P. Parker, S. M. Simon, S. T. Staggs, C. Visnjic, E. Wollack, K. U.-Yen, K. W. Yoon, and Y. Zhao, "Planar orthomode transducers for feedhorn-coupled tes polarimeters," *AIP Conference Proceedings*, vol. 1185, pp. 490–493, 12 2009.
 - [12] P. S. Barry, A. Anderson, B. Benson, J. E. Carlstrom, T. Cecil, C. Chang, M. Dobbs, M. Hollister, K. S. Karkare, G. K. Keating, D. Marrone, J. McMahon, J. Montgomery, Z. Pan, G. Robson, M. Rouble, E. Shirokoff, and G. Smecher, "Design of the SPT-SLIM Focal Plane: A Spectroscopic Imaging Array for the South Pole Telescope," *Journal of Low Temperature Physics*, vol. 209, pp. 879–888, Dec. 2022.
 - [13] G. Robson, *The focal plane development of SPT-SLIM, an on-chip superconducting filter-bank spectrometer pathfinder for millimetre line intensity mapping*. PhD thesis, Cardiff University, 2024.
 - [14] G. Robson, A. J. Anderson, P. S. Barry, S. Doyle, and K. S. Karkare, "The Simulation and Design of an On-Chip Superconducting Millimetre Filter-Bank Spectrometer," *Journal of Low Temperature Physics*, vol. 209, pp. 493–501, Nov. 2022.
 - [15] T. Cecil, C. Albert, A. J. Anderson, P. S. Barry, B. Benson, C. Cotter, C. Chang, M. Dobbs, K. Dibert, R. Gualtieri, K. S. Karkare, M. Lisovenko, D. P. Marrone, J. Montgomery, Z. Pan, G. Robson, M. Rouble, E. Shirokoff, G. Smecher, G. Wang, and V. Yefremenko, "Fabrication Development for SPT-SLIM, a Superconducting Spectrometer for Line Intensity Mapping," *IEEE Transactions on Applied Superconductivity*, vol. 33, p. TASC.2023, Aug. 2023.
 - [16] E. Shirokoff, P. S. Barry, C. M. Bradford, G. Chattopadhyay, P. Day, S. Doyle, S. Hailey-Dunsheath, M. I. Hollister, A. Kovács, C. McKenney, H. G. Leduc, N. Llombart, D. P. Marrone, P. Mausekopf, R. O'Brient, S. Padin, T. Reck, L. J. Swenson, and J. Zmuidzinas, "MKID development for SuperSpec: an on-chip, mm-wave, filter-bank spectrometer," in *Millimeter, Submillimeter, and Far-Infrared Detectors and Instrumentation for Astronomy VI* (W. S. Holland and J. Zmuidzinas, eds.), vol. 8452 of *Society of Photo-Optical Instrumentation Engineers (SPIE) Conference Series*, p. 84520R, Sept. 2012.
 - [17] K. S. Karkare, P. S. Barry, C. M. Bradford, S. Chapman, S. Doyle, J. Glenn, S. Gordon, S. Hailey-Dunsheath, R. M. J. Janssen, A. Kovács, H. G. LeDuc, P. Mausekopf, R. McGeehan, J. Redford, E. Shirokoff, C. Tucker, J. Wheeler, and J. Zmuidzinas, "Full-Array Noise Performance of Deployment-Grade SuperSpec mm-Wave On-Chip Spectrometers," *Journal of Low Temperature Physics*, vol. 199, pp. 849–857, Feb. 2020.
 - [18] T. Takekoshi, K. Karatsu, J. Suzuki, Y. Tamura, T. Oshima, A. Taniguchi, S. Asayama, T. J. L. C. Bakx, J. J. A. Baselmans, S. Bosma, J. Bueno, K. W. Chin, Y. Fujii, K. Fujita, R. Huiting, S. Ikarashi, T. Ishida, S. Ishii, R. Kawabe, T. M. Klapwijk, K. Kohno, A. Kouchi, N. Llombart, J. Maekawa, V. Murugesan, S. Nakatsubo, M. Naruse, K. Ohtawara, A. Pascual Laguna, K. Suzuki, D. J. Thoen, T. Tsukagoshi, T. Ueda, P. J. de Visser, P. P. van der Werf, S. J. C. Yates, Y. Yoshimura, O. Yurduseven, and A. Endo, "DESHIMA on ASTE: On-Sky Responsivity Calibration of the Integrated Superconducting Spectrometer," *Journal of Low Temperature Physics*, vol. 199, pp. 231–239, Feb. 2020.
 - [19] Z. Pan, *A Measurement of Gravitational Lensing of the Cosmic Microwave Background Using SPT-3G*. PhD thesis, University of Chicago, 2020.
 - [20] S. P. Davis, M. C. Abrams, and J. W. Brault, *Fourier transform spectrometry*. Academic press, 2001.
 - [21] Z. Pan, P. S. Barry, T. Cecil, C. Albert, A. N. Bender, C. L. Chang, R. Gualtieri, J. Hood, J. Li, J. Zhang, M. Lisovenko, V. Novosad, G. Wang, and V. Yefremenko, "Measurement of dielectric loss in silicon nitride at centimeter and millimeter wavelengths," *IEEE Transactions on Applied Superconductivity*, vol. 33, no. 5, pp. 1–7, 2023.
 - [22] K. Dibert and the SPT-SLIM Collaboration, "The On-sky Atmospheric Calibration of SPT-SLIM," *IEEE Transactions on Applied Superconductivity*, 2025. Submitted August 2025.